

Modeling of the Formation of AlN Precipitates During Solidification of Steel

D. Kalisz*, S. Rzadkosz

AGH University of Science and Technology,
Reymonta 23, 30-059 Kraków, Poland

* Corresponding author. E-mail address: dorotkapo@yahoo.com

Received 13.07.2012; accepted in revised form 04.09.2012

Abstract

The study was carried out computer simulations of the formation process of AlN precipitates in the solidification of steel. The chemical composition of steel and non-metallic inclusions formed was determined using the commercial software FactSage. Calculated amount of precipitates formed during cooling of steel between the liquidus and solidus temperatures under conditions of thermodynamic equilibrium. In parallel, the computations were performed using your own computer program. It was found that aluminum nitride is formed at the final stage of solidification, and the condition of its formation is low oxygen content in steel.

Keywords: Computer simulation, Aluminum nitride, Solidification of steel, Continuous casting of steel, Silicon steel

1. Introduction

Formation of non-metallic inclusions in steel ingot obtained in continuous casting machine (CCS) is a complex process. The chemical composition, size and spatial distribution influence the structure and properties of cast ingot. The initial non-metallic inclusions resulting from steel de-oxidization are in major part removed in ladle, mainly during argon purging and the remainder should be removed in castin tundish. In the ideal case, the steel tapped into the casting mould might be almost inclusions free. However, in casting mold new inclusions are produced in liquid steel for two reasons: decrease of equilibrium solubility product with decreasing temperature and segregation of liquid steel components at the solidification front. These secondary inclusions may play an important role in structure formation. The development of technology of steel refining in ladle and casting tundish, so called tertiary metallurgy, allows for assure the relevant conditions for required structure and properties of the ingot. In high grade steels and specific purpose steels the kind of emerging inclusions, their chemical composition, dimensions and

total amount are crucial for optimal steel properties. The present work deals with the process of AlN precipitates formation during steel solidification. The AlN play very important role in steel structure formation, which is particularly important in obtaining high magnetic properties of grain oriented high silicon steel [1]. As aluminum shows high chemical affinity to both oxygen and nitrogen in steel, the correct determination of the conditions favourable for AlN formation is rather complicated task [2], [3] [4], [5]. The aim of the present work was the computer simulation of steel components distribution between phases, with special focus on AlN formation. The obtained results are verified with the results of steel sample analysis by means of transmission electron microscopy.

2. The object of research

The simulation of AlN precipitation in the course of steel solidification in continuously cast ingot was carried out for high silicon grain oriented steel (Polish designation ETZ), assigned for

electric transformer core. The structure active aluminum nitride forms in the solid state, what requires sufficient levels of aluminum and nitrogen in steel. AlN precipitated from liquid steel is worthless as structure forming agent, as it either floats out from liquid steel, or, if remains, has too big size to effectively pin the grain boundaries. The steel composition adopted for the calculations is given in Table 1. It was obtained from chemical analysis of the sample taken from casting tundish.

Table 1.
Chemical composition of steel adopted in the calculations

Chemical composition of steel [mass pct.]									
C	Mn	Si	P	S	Cu	Al	N	O	
1	0,037	0,24	3,01	0,01	0,01	0,45	0,015	0,0125	0,00465
2	0,041	0,24	3,0	0,014	0,009	0,42	0,0092	0,0097	0,00181

The computer simulation was performed in two ways: first using the commercial software FactSage and next using the simple program built for this very purpose. In order to verify the results of simulations the samples taken from steel ingot were examined by means of transition electron microscopy.

3. The simulation of AlN formation in steel with the use of FactSage

Secondary non-metallic inclusions emerge during the crystallization of steel in continuous casting mould, and to some extent in the still liquid core of the ingot in the secondary cooling zone out of the mould. The necessary condition of inclusion formation is to reach the sufficient concentrations of both inclusion forming components (e.g. aluminum and nitrogen) [6]. For given temperature the inclusion forms, if the solubility product $[Al][N]$, which follows from the equilibrium constant of reaction:



gdzie:

$$K = \frac{a_{AlN}}{a_{Al}a_N} = \frac{a_{AlN}}{[Al]f_{Al}[N]f_N} \quad (2)$$

The aluminum and nitrogen activities in steel depend on its composition and temperature. During steel solidification various non-metallic compounds are formed, i.e. oxides, nitrides or sulphides, which may constitute non-metallic phase or exist as separate inclusions. This depends also on physical conditions of inclusions flotation and bonding in slag phase.

The determination of the amount of emerging AlN requires the consideration of thermodynamic equilibrium in the system: liquid steel – non-metallic phase. State of the thermodynamic equilibrium in the system is described with the set of parameters, which basically are: temperature, pressure, and mass of each components in all phases. The masses of components may be easily converted into mass percent or molar fractions. To determine this set of system parameters, under assumed total masses of components in the system, two procedures may be considered:

- evaluation of minimum value of Gibbs free enthalpy of the whole system for variable system parameters,
- solution of set of equilibrium constants of possible chemical reactions in the system, which describe the exchange of components between phases.

In both cases the dependencies of phase composition on the components activities or partial molar Gibbs free enthalpies must be known. The first of the above procedures is employed in commercial programs as FactSage or Thermocalc, the other may be employed in calculations for simpler systems.

In the present work the formation of AlN inclusions in the system Fe-Al-N-O was first considered. The influence of oxygen level in steel on AlN formation is strong, as oxygen and nitrogen compete in formation the compounds with aluminum: Al₂O₃ and AlN. This means, that reaching the proper amount of AlN in steel requires very precise setting of its chemical composition [7], [8].

The calculations of the inter – phase equilibrium parameters in the system liquid steel – non-metallic inclusions were carried out for steel compositions given in Table 1. The temperatures of liquidus and solidus were calculated from relations (3) and (4):

$$T_L = 1809 - \{100,3[\%C] - 22,4[\%C]^2 - 0,16 + 13,55[\%Si] - 0,64[\%Si]^2 + 5,82[\%Mn] + 0,3[\%Mn]^2 + 4,2[\%Cu]\}$$

$$T_K = 1809 - \{415,5[\%C] + 12,3[\%Si] + 6,8[\%Mn] + 124,5[\%P] + 183,9[\%S] + 4,1[\%Al]\}$$

The fraction of solid phase f_s in each calculation step was calculated from the relation:

$$f = \frac{T_L - T}{T_0 - T} \cdot \frac{T_0 - T_i}{T_L - T_i} \quad (5)$$

where T denotes the temperature of respective calculation step.

The equilibrium crystallization of steel was assumed in the calculations, what allowed to express the mass of component in the solid phase as a function of the solid fraction f_s :

$$m_i(s) = m_i(l) \cdot \frac{k \cdot f_s}{1 - f_s + k \cdot f_s} \quad (6)$$

where:

$m_i(s)$ – mass of component „i” in solid phase

$m_i(l)$ – mass of component “i” remained in liquid phase

The composition of metal phase as well as that of inclusions was calculated by means of FactSage software. From the equations (5) and (6) the fraction of solid phase and the concentration of steel components in solid and liquid phase were determined. The procedure was repeated for each calculation step, until the last fragment of liquid solidified. As a results of simulations, the solid phase fraction, mass of emerged Al₂O₃ and AlN inclusions as well as micro-segregation of Al, N and O during of solidification of steel 1 and 2 were determined.

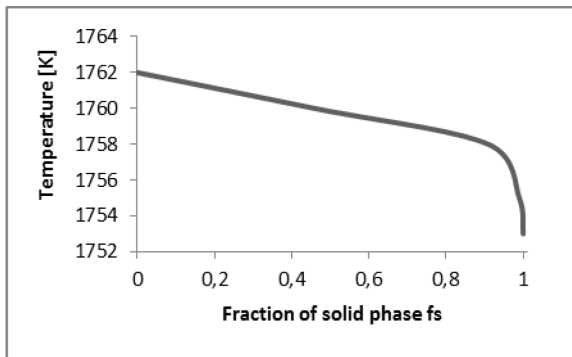


Fig. 1. The fraction of solid phase f_s during solidification of steel nr. 1

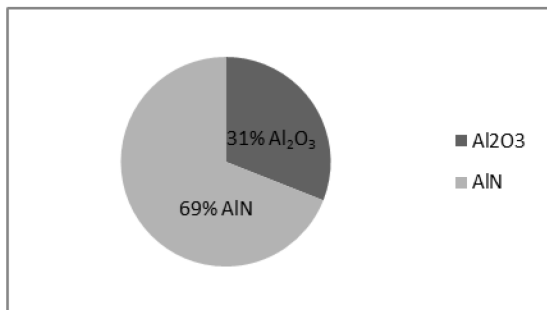


Fig. 2. The composition of aluminum based non-metallic inclusions formed in the course of steel nr 1 solidification

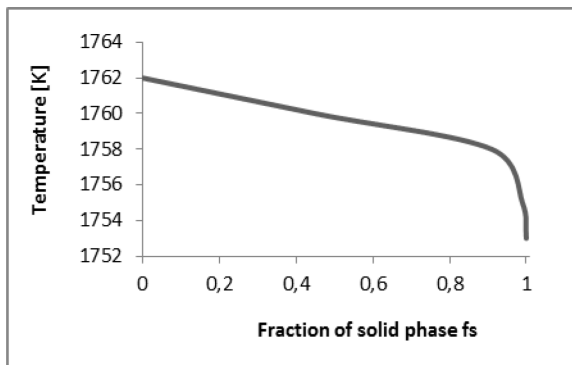


Fig. 3. The fraction of solid phase f_s during solidification of steel nr. 2

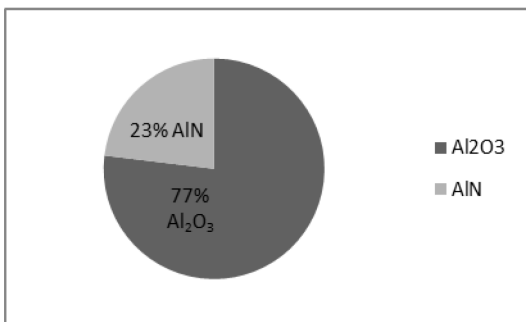


Fig. 4. The composition of aluminum based non-metallic inclusions formed in the course of steel nr 2 solidification

4. Simulation of the process of AlN formation by means of simple program including micro-segregation

The model of Matsumiya et al [9] was adopted to simulate the micro-segregation of steel components. Model includes the process of inclusions formation with simultaneous components micro-segregation during solidification, what makes the simulation more realistic. The program used in this study determines the concentration of components in liquid phase in each step of calculations, and controls the resulting current value of solubility product. If the inclusion have precipitated, the concentrations of liquid metal components are corrected, i.e. lowered [3], [6], [10].

The current temperature of solid – liquid interface varies according to the relation:

$$T = T_0 - \frac{T_0 - T_K}{1 - f_S \cdot \frac{T_L - T_K}{T_0 - T_K}} \quad (7)$$

where:

T – current temperature of solid – liquid interface,

T_0 – melting temperature of pure iron,

T_L – liquidus temperature of steel,

T_K – temperature of the end of solidification, i.e. the solidus temperature for the composition of final portion of freezing steel.

The progress of the process of steel solidification may be related either to fraction of solid phase or to time. The relation between solid fraction and time is expressed with parabolic law:

$$\frac{df_s}{dt} \propto \frac{1}{\sqrt{t}} \quad (8)$$

Subsequent portions of solidifying liquid, corresponding to calculation domains, have higher concentration of dissolved steel components. For this reason the back diffusion in solid phase may be observed, directed towards the mould walls. The resulting concentration gradient in steel may be described with II Fick's law:

$$\frac{\partial C}{\partial t} = D_i \cdot \frac{\partial^2 C}{\partial x^2} \quad (9)$$

In the liquid phase the homogenization caused by diffusion is much faster than diffusion in solid, what justifies the assumption of uniform components concentration in liquid [11], [12], [13].

The calculated progress of crystallization of steel nr 1 was presented in fig. 5, as a dependence between solid fraction and the temperature. This plot takes into account the AlN precipitation. Without precipitation the lower value of final temperature of solidification T_K would be obtained. The activity of AlN in the solid inclusions was assumed 0.2.

The calculations cycle was terminated at the value $f_s = 0.99$. Due to the minimal amount of liquid further proceeding has no physical meaning.

The solidification range is 1770 K – 1655 K for cooling rate 100 K/min and 1770 K – 1645 K for the rate 500 K/min. The lower temperature value of solidification end at higher cooling rate results from the reduction of back – diffusion in solid. In the industrial practice the cooling rate of the ingot is within the range 100 – 500 K/min [14], [15], [16], [17], [18].

Figs 7 and 8 present the change of aluminum concentration in liquid steel nr 1 (Table 1) in the course of crystallization for two values of cooling rate. It grows from the initial value 0.015 % up to 0.05 %. At the cooling rate 500 K/min the distinct bend may be seen at the curve, which corresponds to AlN precipitation. At cooling rate 100 K/min such a bend is not observed. Figs 9 and 10 demonstrate the variation of nitrogen concentration in the course of crystallization. During the process the concentration of nitrogen grows more than two times from the initial value 0.0125 %.

At the cooling rate 500 K/min the decrease of nitrogen concentration close to the end of crystallization may be observed, due to the AlN formation. This effect corresponds to this described earlier for Al. Figs. 11 and 12 demonstrate the variation of solubility product of AlN. At the cooling rate 100 K/min the real value of solubility product merely approaches the equilibrium one at the highest values of solid fraction. At cooling rate 500 K/min both curves intersect each other. The crosscut point marks the beginning of AlN precipitation during crystallization.

The data obtained in the calculations do not directly illustrate the spatial distribution of inclusions in the structure of the ingot, as the inclusions are not immediately engulfed through moving solidification front. They may gather in the interdendritic space or drift along the solidification front. In the case of silicon steel the inclusions are considerably weakly engulfed with solidification front.

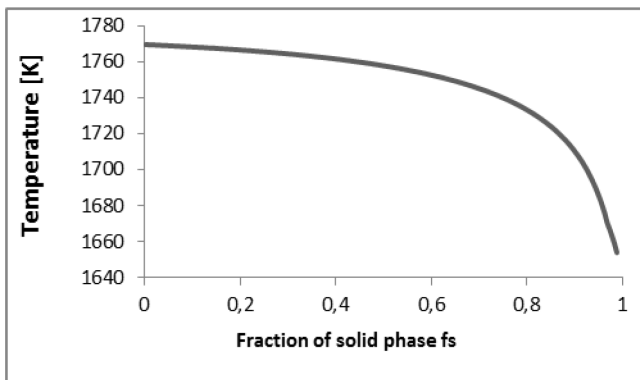


Fig. 5. The temperature variation of calculation domain during solidification within its volume for the steel nr 1, at cooling rate 100 K/min. Assumed activity of AlN in inclusion 0.2

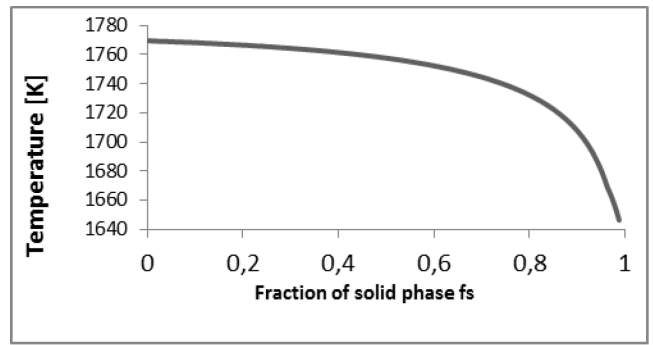


Fig. 6. The temperature variation of calculation domain during solidification within its volume for the steel nr 1, at cooling rate 500 K/min. Assumed activity of AlN in inclusion 0.2

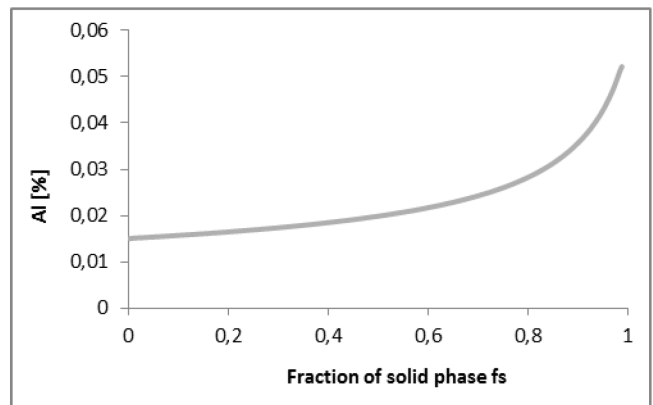


Fig. 7. Micro-segregation of Al during solidification of steel nr 1 at the cooling rate 100 K/min

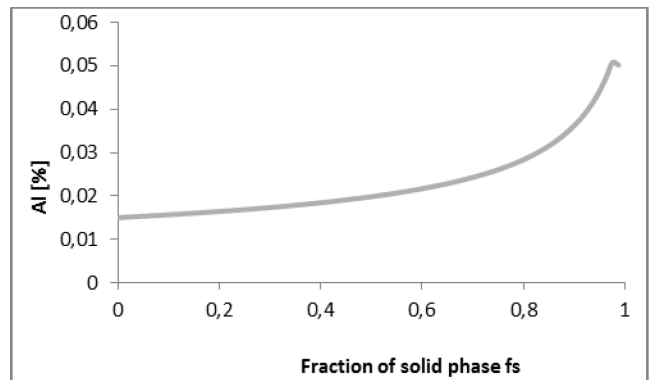


Fig. 8. Micro-segregation of Al during solidification of steel nr 1 at the cooling rate 500 K/min

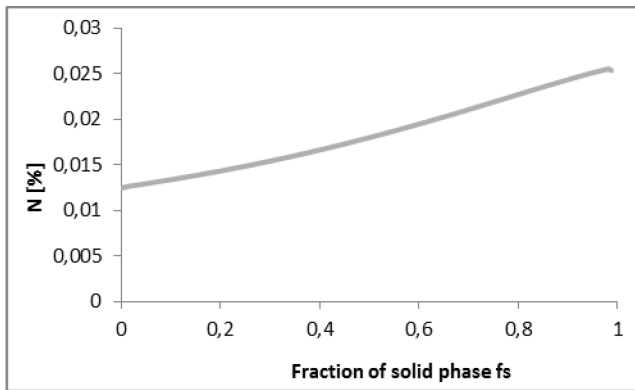


Fig. 9. Micro-segregation of N during solidification of steel nr 1 at the cooling rate 100 K/min

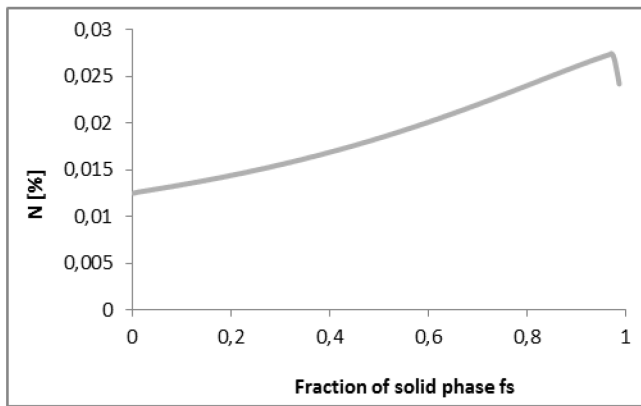


Fig. 10. Micro-segregation of N during solidification of steel nr 1 at the cooling rate 500 K/min

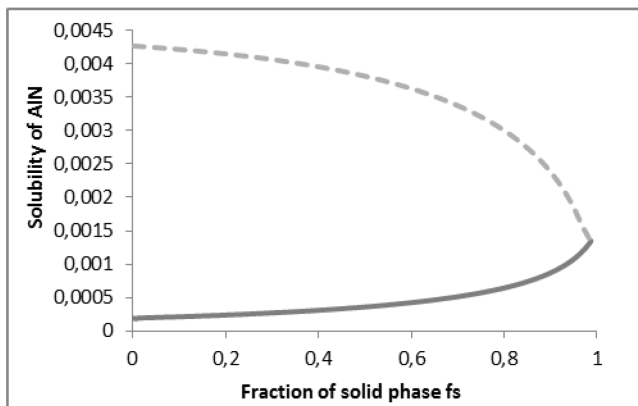


Fig. 11. Comparison of equilibrium value of solubility product of AlN with the actual value at the cooling rate 100 K/min

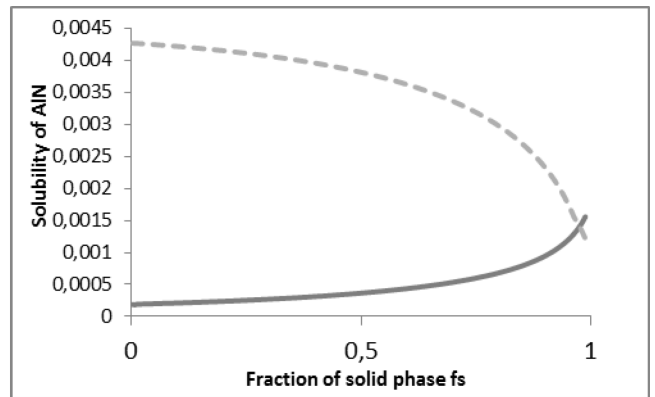


Fig. 12. Comparison of equilibrium value of solubility product of AlN with the actual value at the cooling rate 500 K/min

5. Non – metallic phase in silicon steel

The examination of silicon steel microstructure were carried out with the aim of determination the chemical composition and dimension of second phase precipitates, which are formed during steel solidification. The methods of transmission electron microscopy and X-ray microanalysis were used. In the examinations special attention was directed towards identification of diverse inclusions particles of various chemical composition. For this reason the samples were examined with optical microscope prior to TEM studies. Fig 13 presents the microstructure of silicon steel obtained in transmission electron microscope. The AlN precipitate of the size approximately 0.5 μm is visible. The results of point microanalysis from the precipitate area are given below. Table 2 gives the chemical composition deduced from X-ray microanalysis. It may be deduced from the presence of Al, N and Si, that AlN is main component of precipitate, and oxides of aluminum and silicon are also present.

Table 2.

Chemical composition of AlN precipitate area deduced from X-ray microanalysis

Pierwiastek	[mass pct.]	[atom pct.]
N	2,0	6,4
N	3,5	9,6
O	2,2	5,4
Al	3,2	4,6
Si	17,3	24,0
S	0,3	0,4
Ti	0,0	0,0
Mn	7,2	5,1
Fe	59,1	41,2
Cu	5,3	3,2
Suma	100	100

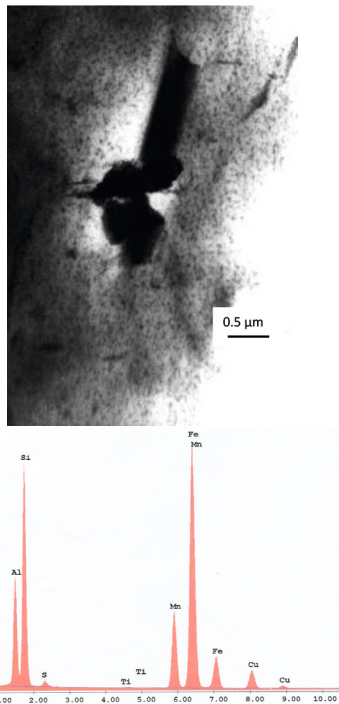


Fig. 13. The microstructure of silicon transformer steel (nr 1) obtained in transmission electron microscope with AlN precipitate visible. The results of point microanalysis from the precipitate area are given below

6. Conclusions

The AlN precipitates play important role in silicon transformer steel technology. These are formed in the course of steel solidification, and later during steel cooling after hot rolling. During the process of steel solidification, in dependence of its composition and cooling rate, the AlN based precipitates of various dimensions and space distribution may be formed. The chemical composition of the precipitates is also of importance, as they contain oxides of silicon and aluminum besides dominant component AlN. The simulation procedure adopted in the present work may be useful in the control of behaviour of AlN based non-metallic precipitates, and, in consequence, in determination the optimum process parameters.

Acknowledgments

This work was done in the contract: 11.11.170.318

References

[1] Morita, Z., Tanaka, T. & Yanai, T. (1987). Equilibria of Nitride Forming Reactions in Liquid Iron Alloys. *Met. Trans. B*, 18B, 195-202.

[2] Suzuki, M., Yamaguchi, R., Murakami, K. & Nakada, M. (2001). Inclusion Particle Growth during Solidification of Stainless Steel. *ISIJ Int.* 41, 247-256.

[3] Liu, Z., Gu, K. & Cai, K. (2002). Mathematical Model of Sulfide Precipitation on Oxides during Solidification of Fe-Si Alloy. *ISIJ Int.* 42, 950 – 957.

[4] Kobayashi S. (1999). Thermodynamic Fundamentals for Alumina Content Control of Oxide Inclusions in Mn-Si Deoxidation of Molten Steel, *ISIJ Intern.* 39, 664-670.

[5] Wolczyński, W. (2002). *Effect of the back-diffusion onto doublet structure formation and solute redistribution within alloys solidifying directionally, with or without convection*, Polish Academy of Sciences, Institute of Metallurgy and Materials Science, Kraków.

[6] Ma, Z. & Janke, D (1986). Characteristics of Oxide Precipitation and Growth during Solidification of Deoxidized Steel. *ISIJ Intern.* 38, 46-52.

[7] Płaczek, K., Kalisz, D. & Wypartowicz, J. (2004). Problemy matematycznego modelowania mikrosegregacji składników i wydzielania wtrąceń niemetalicznych podczas krzepnięcia stali. II Międzynar. Konf. Ciągłe Odlewanie Stali, 16-18 June 2004, Krynica, Poland, 265-274.

[8] Goto, H., Miyazawa, K., Yamada, W. & Tanaka K. (1995). Effect of Cooling Rate on Composition of Oxides Precipitated during Solidification of Steel. *ISIJ Int.* 35, 708 – 714.

[9] Matsumiya, T., Kajioaka, H., Mizoguchi, S., Ueshima, Y. & Esaka, H. (1984). Mathematical Analysis of segregation in continuously cast slabs. *Trans. ISIJ.* 24, 873-882.

[10] Liu, Z., Wei, J. & Cai, K. (2002). A Coupled Mathematical Model of Microsegregation and Inclusion Precipitation during Solidification of Silicon Steel. *ISIJ Int.* 42, 958 – 963.

[11] Brody, H.D., Flemings, M.C. (1966). Solute Redistribution in Dendritic Solidification. *Trans. Met. Soc. AIME.* 236, 615-624.

[12] Clyne, T. W. & Kurz, W. (1981). Solute Redistribution During Solidification with Rapid Solid State Diffusion. *Met. Trans.* 12A, 965-971.

[13] Ohnaka, I. (1986). Mathematical Analysis of Solute Redistribution During Solidification with Diffusion in Solid Phase. *Trans. ISIJ.* 26, 1045-1051.

[14] Kobayashi, S., Nagamichi, T. & Gunji, K (1988). Numerical Analysis of Solute Redistribution during Solidification Accompanying δ/γ Transformation. *Trans. ISIJ.* 28, 543-552.

[15] Wypartowicz, J. & Kalisz, D. (2004). Kontrola wydzielenia siarczokowych i azotkowych w produkcji blachy transformatorowej o zorientowanym ziarnie. *Hutnik.* 71(6), 259-264.

[16] Suzuki, M., Yamaguchi, R., Murakami, K. & Nakada, M. (2001). Inclusion Particle Growth during Solidification of Stainless Steel. *ISIJ Int.* 41, 247-256.

[17] Wypartowicz, J. & Kalisz, D (2005). Oddziaływanie wtrąceń niemetalicznych w stali z postępującym frontem krzepnięcia. *Hutnik.* 72(1), 2-6.

[18] Kalisz, D. & Wypartowicz, J. (2004). Behaviour of non-metallic particles during solidification of silicon steel, Metal 2004, 13 Międzynar. Konf. Hradec n. Moravici.